

Vapor–Liquid Equilibrium Data for the Sulfur Dioxide (SO₂) + Difluoromethane (R32) System at Temperatures from 288.07 to 403.16 K and at Pressures up to 7.31 MPa

A. Valtz,¹ C. Coquelet,¹ and D. Richon^{1,2}

Received March 8, 2004

Isothermal vapor–liquid equilibrium data have been measured for the binary system R32 (difluoromethane)+SO₂ at eight temperatures between 288.07 and 403.16 K, and at pressures in the range 0.417–7.31 MPa. The experimental method used in this work is of the static–analytic type, taking advantage of two pneumatic capillary samplers (RolsiTM, Armines' patent) developed in the CENERG/TEP laboratory. The data were measured with uncertainties within ± 0.02 K and ± 0.0015 MPa, respectively, for temperatures and pressures and $\pm 1\%$ for molar compositions as a result of careful calibrations. The isothermal P, x, y data are well represented with the Peng–Robinson equation of state using the Mathias–Copeman alpha function and the Wong–Sandler mixing rules involving the NRTL model.

KEY WORDS: critical point; difluoromethane; high pressures; modeling; refrigerants; sulfur dioxide; supercritical gas solubility; VLE data.

1. INTRODUCTION

Industry needs new fluids to replace refrigerants implicated in ozone destruction such as chlorofluorocarbons (CFCs) or hydrochlorofluorocarbons (HCFCs). Refrigerant use, production, and distribution are governed by modifications of the 1987 Montreal Protocol. CFCs are prohibited since 1996 for member countries, and the deadline for HCFCs, which have lower ozone depletion potential, is 2030.

¹Centre d'Energétique, Ecole Nationale Supérieure des Mines de Paris CENERG/TEP, 35 Rue Saint Honoré, 77305 Fontainebleau, France.

²To whom correspondence should be addressed. E-mail: dominique.richon@ensmp.fr

In this paper, we are concerned with the study of a new system composed of a hydrofluorocarbon (R32) and an old refrigerant (SO₂). SO₂ was used, like ammonia, in industrial refrigeration applications, and it has zero ozone depletion potential.

An accurate knowledge of the thermophysical properties of alternative refrigerants, like mixtures containing HFCs, is necessary to evaluate the performance of refrigeration cycles. The importance of vapor–liquid equilibria (VLE) was stressed during the second IUPAC Workshop (April 9–11, 2001) on refrigerants (Ecole des Mines, Paris, France) and the third IUPAC Workshop held during the ICCT conference (July 28–August 2, 2002, Rostock, Germany).

The CENERG/TEP laboratory has already published several sets of VLE data concerning different mixtures with R32, R227ea, propane, and CO₂ [1–5]. The R227ea + SO₂ system, as shown in a previous study [6], displays an anomalous behaviour of the azeotropic line at temperatures above the R227ea critical temperature. Nothing similar is displayed by VLE data presented for the R32–SO₂ system at four temperatures below the R32 critical temperature (288.07, 303.16, 323.15, and 343.15 K) and at four temperatures above (353.15, 363.15, 383.18, and 403.16 K).

The experimental results have been fitted using the Peng–Robinson equation of state (PR EoS). Finally, we present the pure component vapour pressure curves along with the predicted mixture critical line using the parameters adjusted on binary VLE data.

2. EXPERIMENTAL

2.1. Materials

SO₂ was obtained from Aldrich with a certified purity higher than 99.9 vol%. R32 was purchased from DEHON (France) and has a certified purity higher than 99.99 vol%. No further purification was performed before use.

2.2. Apparatus

The apparatus used in this work is based on a static–analytic method with liquid and vapor phase sampling. This apparatus is similar to that described by Laugier and Richon [7] and Valtz et al. [1,2].

The equilibrium cell is immersed inside a regulated liquid bath. Temperatures are measured with two platinum resistance thermometer probes (Pt100) inserted inside the equilibrium cell. These Pt100 probes are calibrated against a 25 Ω Reference probe (Tinsley Precision Instrument)

certified by the Laboratoire National d'Essais (Paris) following the International Temperature Scale 1990 protocol.

Pressures are measured using a pressure transducer (Druck, Type PTX611, range: 0–6 MPa). This sensor was calibrated against a dead-weight pressure balance (5202S Model from Desgranges and Huot).

Pressure and temperature data acquisition is performed with a computer linked to an HP unit (HP34970A). The resulting estimated uncertainties in this work are ± 0.02 K and ± 0.0015 MPa.

The analytical work was carried out using a gas chromatograph (Varian Model CP-3800) equipped with a thermal conductivity detector (TCD) connected to a data acquisition system driven by Borwin software (Version 1.5, from JMBS, France). The analytical column is Haysep T Model, 100/120 mesh (3.2 mm silcosteel tube, 1.6 m length, from Resteck, France). The TCD was repeatedly calibrated by introducing known amounts of each pure compound through a syringe in the injector of the gas chromatograph. Taking into account the uncertainties due to calibrations and dispersions of analyses, resulting uncertainties for vapor and liquid mole fractions are estimated to be less than $\pm 1\%$.

2.3. Experimental Procedure

At room temperature, the equilibrium cell and its loading lines are evacuated down to 0.1 Pa. The cell is first loaded with liquid SO₂ (about 5 cm³). Equilibrium temperature is assumed to be reached when the two Pt100 probes give equivalent temperature values within their temperature uncertainty for at least 10 min. After recording the vapor pressure of SO₂ (the heavier component) at an equilibrium temperature, the two-phase envelopes are described with about six P, x, y points (liquid and vapor). R32 (the lighter component) is then introduced step by step, leading to successive equilibrium mixtures of increasing overall R32 content. Equilibrium is assumed when the total pressure remains unchanged within ± 1.0 kPa during a period of 10 min under efficient stirring.

For each equilibrium condition, at least five samples of both vapor and liquid phases are withdrawn using the pneumatic samplers RolsiTM [8] and analyzed in order to check for measurement repeatability.

3. CORRELATIONS

The critical temperatures (T_C), critical pressures (P_C), and acentric factors (ω), for each of the two pure compounds are provided in Table I. Our experimental VLE data are correlated by means of TepThermsoft in-house software. We have used the PR EoS [9] to correlate the data.

Table I. Critical Parameters and Acentric Factors [19]

Compound	T_c (K)	P_c (MPa)	ω
R32	351.55	5.8310	0.271
SO ₂	430.80	7.8831	0.2510

To have accurate representation of vapor pressures of each component, we use the Mathias–Copeman alpha function [10] with three adjustable parameters (Eqs. (1) and (2)), which was especially developed for polar compounds.

$$\alpha(T) = \left[1 + c_1 \left(1 - \sqrt{\frac{T}{T_c}} \right) + c_2 \left(1 - \sqrt{\frac{T}{T_c}} \right)^2 + c_3 \left(1 - \sqrt{\frac{T}{T_c}} \right)^3 \right]^2 \quad (1)$$

if $T < T_c$ and

$$\alpha(T) = \left[1 + c_1 \left(1 - \sqrt{\frac{T}{T_c}} \right) \right]^2 \quad (2)$$

if $T \geq T_c$,

c_1 , c_2 , and c_3 are adjustable parameters.

To lead to the best representation of mixture VLE, we chose the Wong–Sandler (WS) mixing rules [11], based on the Huron–Vidal approach.

$$b = \frac{\sum_i \sum_j x_i x_j (b - (a/RT))_{ij}}{1 - \left(\left(\sum_i x_i (a_i/b_i)/RT \right) + (A^E(T, P = \infty, x_i)/CRT) \right)}, \quad (3)$$

$$b - \frac{a}{RT} = \sum_i \sum_j x_i x_j \left(b - \frac{a}{RT} \right)_{ij}, \quad (4)$$

$$\left(b - \frac{a}{RT} \right)_{ij} = \frac{1}{2} \left[\left(b - \frac{a}{RT} \right)_i + \left(b - \frac{a}{RT} \right)_j \right] (1 - k_{ij}), \quad (5)$$

k_{ij} is a binary interaction parameter.

The excess Gibbs energy model chosen is the NRTL [12] local composition model.

$$\frac{g^E(T, x_i)}{RT} = \sum_i x_i \sum_j \frac{x_j \exp(-\alpha_{ji}(\tau_{ji}/RT))}{\sum_k x_k \exp(-\alpha_{ki} \frac{\tau_{ki}}{RT})} \tau_{ji}, \quad (6)$$

$\tau_{jj} = 0$ and $\alpha_{ii} = 0$.

$\tau_{ji} \neq \tau_{ij}$ while $\alpha_{ij} = \alpha_{ji}$,

α_{ij} , τ_{ji} , and τ_{ij} are adjustable parameters. It is recommended [12] to use $\alpha_{ij} = 0.3$ for systems like the one treated here. τ_{ji} and τ_{ij} are adjusted directly on VLE data through a modified Simplex algorithm [13] using the objective function:

$$F = \frac{100}{N} \left[\sum_1^N \left(\frac{P_{\text{exp}} - P_{\text{cal}}}{P_{\text{exp}}} \right)^2 + \sum_1^N \left(\frac{y_{\text{exp}} - y_{\text{cal}}}{y_{\text{exp}}} \right)^2 \right], \quad (7)$$

where N is the number of data points, P_{exp} is the measured pressure, P_{cal} is the calculated pressure, and y_{exp} and y_{cal} are, respectively, the measured and calculated vapor phase mole fractions.

4. RESULTS AND DISCUSSION

4.1. Vapor Pressures

The Mathias–Copeman (MC) parameters from Component Plus [5] are used to calculate the vapour pressures of R32 (Table II). The MC parameters for SO₂ are determined by an adjustment on experimental values and presented in Table II. The SO₂ experimental vapor–pressure data and the calculated values are presented in Table III showing deviations of less than 0.3%. In previous work [5], we used the R32 MC parameters from Component Plus [20] and observed deviations between experimental and calculated vapour pressures of less than 0.3%.

4.2. Vapor–Liquid Equilibria of the R32 (1)–SO₂(2) System

Experimental and calculated VLE data are reported in Table IV and plotted in Fig. 1. The adjusted parameters corresponding to the WS mixing rules involving the NRTL model, applied to PR EoS, are given in Table V. The trend with temperature of these binary parameters is plotted in Figs. 2–4.

Table II. Mathias–Copeman Coefficients

Coefficients	R32 [5]	SO ₂
c_1	0.8219	0.7696
c_2	−0.3977	−0.3756
c_3	0.7622	1.4480

Table III. Experimental and Calculated Vapor Pressures for SO₂

T (K)	P_{exp} (MPa)	P_{cal} (MPa)	ΔP (MPa)
288.04	0.2761	0.2758	0.0003
288.10	0.2766	0.2764	0.0002
303.15	0.4608	0.4622	-0.0014
323.16	0.8395	0.8407	-0.0012
343.16	1.4175	1.4157	0.0018
353.16	1.7980	1.7943	0.0037
363.15	2.2474	2.2436	0.0038
366.15	2.3970	2.3936	0.0034
374.23	2.8329	2.8351	-0.0022
376.23	2.9528	2.9532	-0.0004
383.14	3.3877	3.3899	-0.0022
403.19	4.9151	4.9356	-0.0205

Table IV. Vapor-liquid Equilibrium Pressures and Phase Compositions for R32 (1)-SO₂(2) Mixtures (ΔP is the deviation in pressure; Δy is the deviation in vapor mole fraction)

P_{exp} (MPa)	x_1	$y_{1,\text{exp}}$	P_{cal} (MPa)	$y_{1,\text{cal}}$	ΔP (MPa)	Δy
288.07 K						
0.4170	0.135	0.401	0.4166	0.408	0.0004	-0.007
0.5260	0.233	0.563	0.5214	0.567	0.0046	-0.004
0.6219	0.333	0.667	0.6248	0.673	-0.0029	-0.006
0.7458	0.456	0.759	0.7469	0.763	-0.0011	-0.004
0.9334	0.651	0.865	0.9311	0.863	0.0023	0.002
1.1136	0.837	0.939	1.1109	0.939	0.0027	0.000
303.16 K						
0.5954	0.084	0.268	0.5899	0.265	0.0055	0.003
0.8039	0.223	0.514	0.8051	0.519	-0.0012	-0.005
1.0134	0.370	0.666	1.0233	0.670	-0.0099	-0.004
1.1985	0.503	0.761	1.2129	0.763	-0.0144	-0.002
1.3903	0.638	0.839	1.4016	0.836	-0.0113	0.003
1.5743	0.767	0.898	1.5827	0.897	-0.0084	0.001
1.7080	0.856	0.936	1.7133	0.937	-0.0053	-0.001
323.15 K						
1.1589	0.139	0.338	1.1569	0.342	0.0020	-0.004
1.4752	0.278	0.534	1.4677	0.536	0.0075	-0.002
1.8289	0.442	0.684	1.8293	0.685	-0.0004	-0.002
2.1343	0.584	0.779	2.1406	0.780	-0.0063	-0.001
2.4500	0.723	0.860	2.4564	0.858	-0.0064	0.001
2.7490	0.848	0.923	2.7554	0.923	-0.0064	0.000

Table IV. (Continued)

P_{exp} (MPa)	x_1	$y_{1,exp}$	P_{cal} (MPa)	$y_{1,cal}$	ΔP (MPa)	Δy
343.15 K						
1.8141	0.123	0.272	1.8078	0.275	0.0063	-0.003
2.3948	0.305	0.516	2.3848	0.519	0.0100	-0.003
2.9028	0.466	0.657	2.8968	0.661	0.0060	-0.005
3.4020	0.618	0.764	3.3973	0.766	0.0047	-0.003
3.8957	0.759	0.854	3.8948	0.852	0.0009	0.002
4.3559	0.881	0.924	4.3710	0.925	-0.0151	0.000
353.15 K						
5.3156	0.880	0.914	5.3116	0.913	0.0040	0.001
2.3055	0.136	0.276	2.3036	0.281	0.0019	-0.005
2.7847	0.263	0.449	2.7744	0.453	0.0103	-0.004
3.2963	0.400	0.584	3.2828	0.589	0.0135	-0.004
3.9585	0.571	0.717	3.9398	0.719	0.0187	-0.003
4.6161	0.729	0.819	4.5995	0.821	0.0166	-0.001
363.15 K						
5.5560	0.727	0.798	5.5426	0.796	0.0134	0.002
4.6142	0.537	0.670	4.6117	0.674	0.0025	-0.004
5.1368	0.646	0.746	5.1344	0.747	0.0024	-0.001
6.0214	0.814	0.846	5.9979	0.846	0.0235	0.000
2.8046	0.129	0.248	2.7920	0.252	0.0126	-0.004
3.3867	0.262	0.424	3.3716	0.432	0.0151	-0.008
3.9758	0.397	0.558	3.9679	0.565	0.0079	-0.007
383.18 K						
4.0084	0.107	0.191	3.9997	0.190	0.0087	0.001
4.4557	0.188	0.298	4.4630	0.301	-0.0073	-0.003
4.9515	0.275	0.394	4.9610	0.398	-0.0095	-0.004
5.4748	0.365	0.480	5.4872	0.482	-0.0124	-0.002
5.9809	0.450	0.550	5.9830	0.548	-0.0021	0.002
6.5893	0.552	0.613	6.5806	0.613	0.0087	-0.000
6.8451	0.596	0.635	6.8283	0.634	0.0168	0.001
403.16 K						
5.3693	0.064	0.102	5.3906	0.101	-0.0213	0.001
5.6653	0.105	0.160	5.6915	0.159	-0.0262	0.001
5.9646	0.147	0.211	5.9926	0.211	-0.0280	0.000
6.3217	0.196	0.267	6.3498	0.266	-0.0281	0.001
6.7114	0.250	0.318	6.7388	0.318	-0.0274	0.000
7.0332	0.296	0.355	7.0577	0.356	-0.0245	-0.001
7.3104	0.337	0.380	7.3401	0.384	-0.0297	-0.004

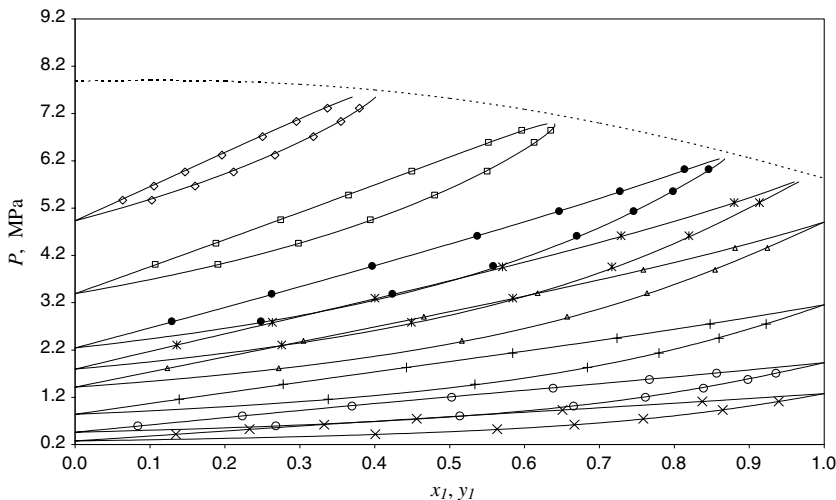


Fig. 1. VLE of the R32 (1)–SO₂ (2) system at different temperatures. × 288.07 K, ○: 303.16 K, +: 323.15 K, Δ: 343.15 K, *: 353.15 K, ●: 363.15 K, □: 383.18 K, ◇: 403.16 K. —: Predicted mixture critical line. Solid lines: Phase envelopes calculated with PR EoS, Wong-Sandler mixing rules, and NRTL activity coefficient model with parameters from Table V.

Table V. Values of the Binary Parameters at Each Temperature

$T(\text{K})$	τ_{12} (J·mol ⁻¹)	τ_{21} (J·mol ⁻¹)	k_{12}
288.07	4189	-13	-0.4073
303.16	4180	-399	-0.3052
323.15	2917	-938	-0.1355
343.15	2416	-1049	-0.0888
353.15	-967	1521	-0.0316
363.15	2485	-1789	-0.0186
383.18	39	70	-0.0024
403.16	1070	-1125	0.0311

The deviations, MRDU and BIASU, applied on pressures and vapor phase mole fractions, are defined by

$$\text{MRDU} = (100/N) \sum |(U_{\text{cal}} - U_{\text{exp}})/U_{\text{exp}}|, \quad (8)$$

$$\text{BIASU} = (100/N) \sum ((U_{\text{exp}} - U_{\text{cal}})/U_{\text{exp}}), \quad (9)$$

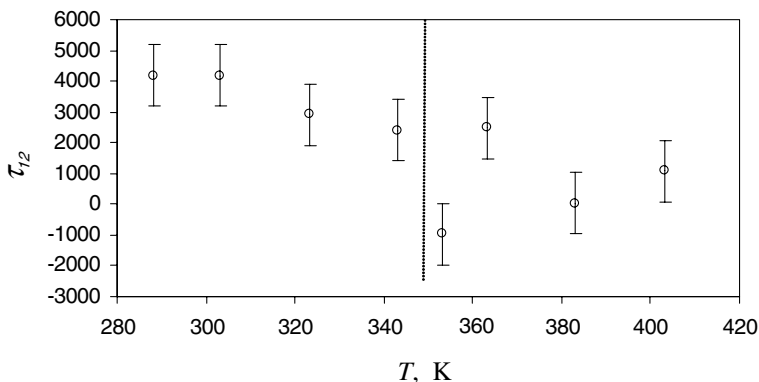


Fig. 2. τ_{12} Binary parameter as a function of temperature. Vertical dashed line represents the R32 critical temperature.

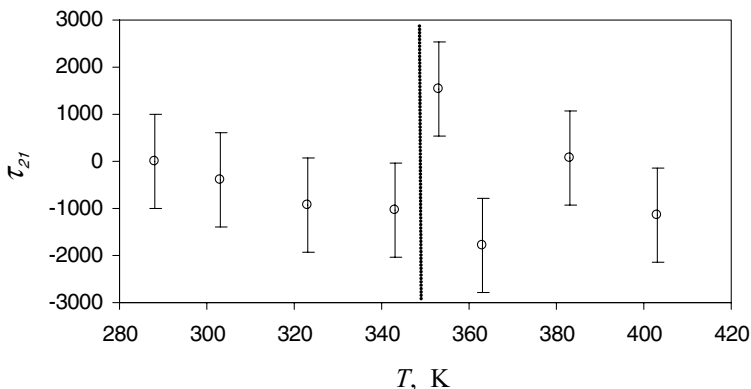


Fig. 3. τ_{21} binary parameter as a function of temperature. Vertical dashed line represents the R32 critical temperature.

where N is the number of data points and $U = P$ or y_1 . These statistical parameters, which give information about the agreement between models and experimental results, are presented in Table VI.

To have an idea of the behavior of this system, a simple thermodynamic model was also used to correlate the experimental data, i.e., the Peng–Robinson EoS with classical mixing rules. Below the R32 critical temperature, this model is as accurate as our recommended model with g^E mixing rules, but it is unable to represent isotherms above the critical temperature. A similar conclusion was also drawn in a previous study [2]. The binary parameters are presented in Table VII. The deviations, MRDU and

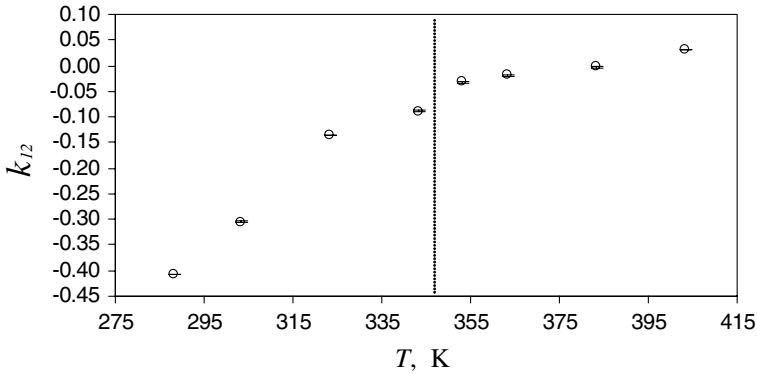


Fig. 4. k_{12} binary parameter as a function of temperature. Vertical dashed line represents the R32 critical temperature.

Table VI. Relative Deviations MRDU and BIASU Obtained in Fitting Experimental VLE Data with PR EoS, Mathias–Copeman Alpha Function, and WS Mixing Rules Involving NRTL Model

$T(K)$	Bias P (%)	MRDP(%)	Bias Y (%)	MRDY(%)
288.07	0.14	0.35	-0.61	0.69
303.16	-0.44	0.70	-0.05	0.50
323.15	-0.02	0.25	-0.27	0.34
343.15	0.13	0.25	-0.40	0.48
353.15	0.29	0.29	-0.66	0.70
363.15	0.26	0.26	-0.75	0.82
383.18	0.00	0.17	-0.20	0.50
403.16	-0.42	0.42	0.09	0.47

BIASU, are also presented in Table VIII. The vapor compositions are not well calculated as the previous model.

A discontinuity in the temperature dependence of the three binary parameters (NRTL and WS) can be identified in Figs. 2–4 close to the R32 critical temperature. Such a discontinuity phenomenon was already described in previous studies [2, 5, 14].

4.3. Critical Line Computation

To calculate the critical line locus at temperatures higher than the critical temperature of R32, it is highly recommended to use

Table VII. Values of the Binary Parameters at Each Temperature for the Peng–Robinson EoS with Classical Mixing Rules

$T(\text{K})$	k_{12}
288.07	-0.00283
303.16	0.00115
323.15	-0.00543
343.15	-0.01035
353.15	-0.01633
363.15	-0.01761
383.18	-0.01789
403.16	-0.01412

Table VIII. Critical Points for the Three Binary Systems

x_1	R32 (1)–SO ₂ (2)		CO ₂ (1)–R32 (2) ^a		CO ₂ (1)–SO ₂ ^b (2)	
	T_{cal} (K)	P_{cal} (MPa)	T_{cal} (K)	P_{cal} (MPa)	T_{cal} (K)	P_{cal} (MPa)
0	430.80	7.883	351.55	5.831	430.80	7.883
0.1	424.47	7.905	348.25	6.196	422.20	8.701
0.2	417.80	7.884	344.47	6.553	412.43	9.442
0.3	410.77	7.817	340.04	6.882	401.36	10.042
0.4	403.37	7.697	336.00	7.187	388.96	10.420
0.5	395.61	7.522	331.09	7.411	375.35	10.494
0.6	387.49	7.289	325.95	7.548	360.94	10.218
0.7	379.02	6.998	320.68	7.598	346.29	9.633
0.8	370.21	6.653	315.33	7.577	331.76	8.864
0.9	361.06	6.262	309.82	7.497	317.51	8.060
1	351.55	5.831	304.20	7.377	304.20	7.377

^aValues from Ref. 5.^bCalculated with PSRK model.

the parameters adjusted to VLE in the corresponding supercritical temperature range (Fig. 5).

Procedures to calculate critical points were proposed by Heidemann and Khalil [15] in 1980 and Michelsen and Heidemann [16] in 1981. They assumed that the stability criterion for an isothermal variation of the molar Helmholtz energy (Eq. (10)) (between an initial state and a very

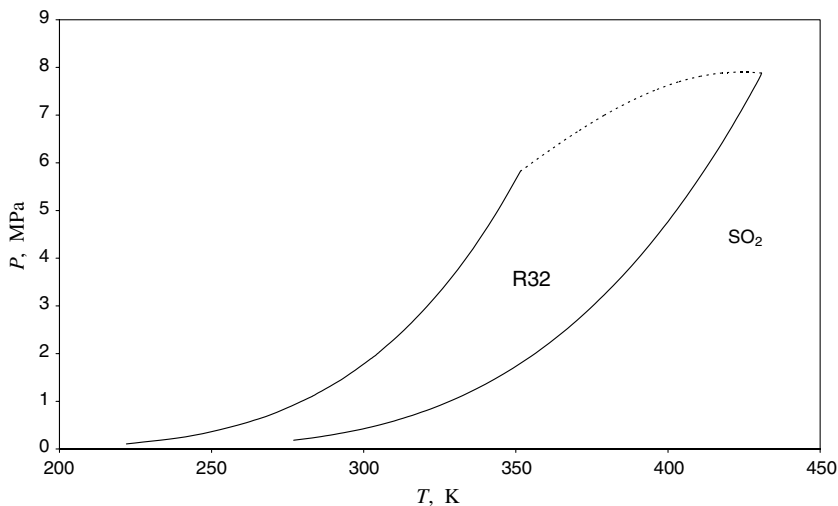


Fig. 5. PT diagram of the R32 + SO₂ system; ---, predicted mixture critical line.

close new one) is expressed by a minimum.

$$A - A^0 - \sum_i \mu_i^0 \Delta n_i \geq 0. \quad (10)$$

The critical point corresponds to the limit of stability. They developed an algorithm to calculate the critical point with a van der Waals type EoS, combined with classical mixing rules. In 1998, Stockfleth and Dohrn [17] improved this method by generalizing the previous algorithm. This improved method was chosen here to calculate the critical line using the PR EoS and WS mixing rules involving the NRTL model. The binary parameters are those obtained by fitting VLE data in the R32 supercritical domain. Results are reported in Table IX and plotted in Fig. 6. We have obtained a predicted critical line locus that is in very good agreement with the isothermal phase envelopes.

4.4. Comparison with CO₂-R32 System

In a previous study, experimental data and modeling on the CO₂-R32 binary system were published [5]. Carbon dioxide is also an old natural refrigerant used in industrial and marine refrigeration. The phase envelope behaviors for CO₂-R32 and R32-SO₂ are similar with no azeotropic point. However, the excess Gibbs enthalpy (see Fig. (7)) reveals a larger

Table IX. Relative Deviations MRDU and BIASU Obtained in Fitting Experimental VLE Data with PR EoS, Mathias–Copeman Alpha Function, and Classical Mixing Rules

$T(\text{K})$	Bias P (%)	MRDP(%)	Bias Y (%)	MRDY(%)
288.07	-1.45	1.48	-2.39	2.39
303.16	-1.79	1.79	-2.18	2.18
323.15	-1.03	1.03	-1.48	1.48
343.15	-0.67	0.67	-1.47	1.47
353.15	0.06	0.11	-1.01	1.03
363.15	0.17	0.17	-0.91	0.95
383.18	0.06	0.22	0.11	0.52
403.16	-0.43	0.44	1.84	1.84

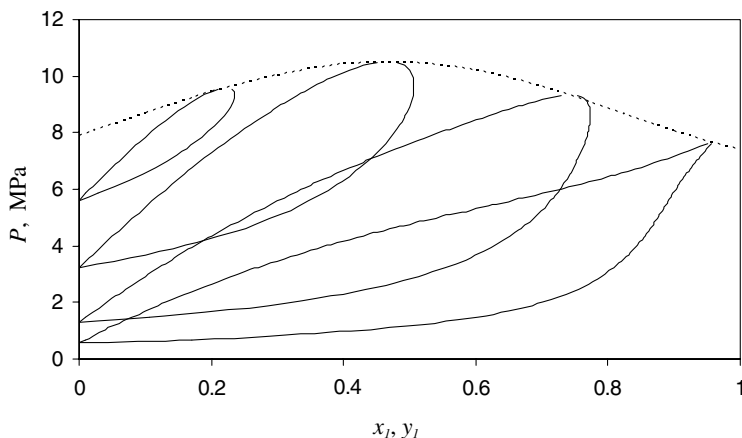


Fig. 6. VLE of the CO₂(1) – SO₂ (2) system at four temperatures, 310, 340, 380 and 410 K, calculated using PSRK predictive model [18]; ---, predicted mixture critical line.

nonideality for the R32–SO₂ system. Ideal mixing is characterized by $G^E = 0$. The R32 and CO₂ molecules lead to “dipole–induced dipole” interactions while the R32 and SO₂ molecules lead to dipole–dipole interactions. Indeed, the R32 dipole moment is 1.97863 D (due to the two fluorine atoms), the SO₂ dipole moment is 1.63087 D (due to the molecular bent resonance structure O=S⁺–O⁻), while CO₂ has a zero dipole moment.

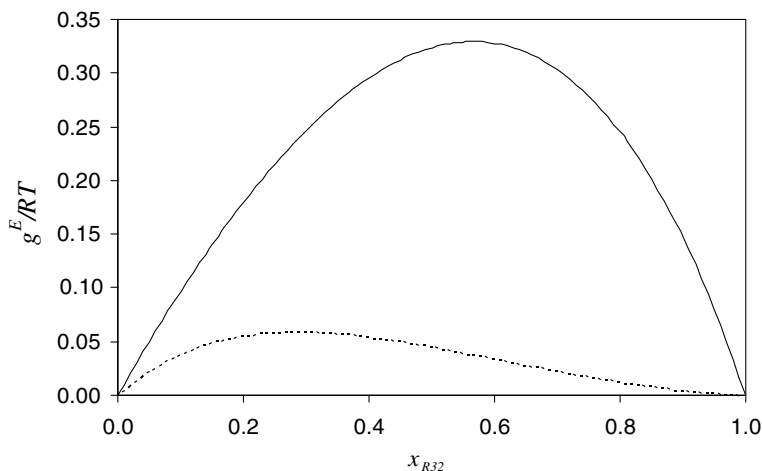


Fig. 7. Excess molar Gibbs enthalpy versus R32 composition for both $\text{CO}_2 + \text{R32}$ (dashed line) and $\text{R32} + \text{SO}_2$ (solid line) systems.

4.5. Study of the Ternary CO_2 – R32 – SO_2 System

It may be interesting to study the behavior of a “new” refrigerant mixture containing R32 (HFC), an old safe refrigerant such as CO_2 and an old hazardous refrigerant such as SO_2 . The predictive model PSRK [18] was used to generate data for the CO_2 – SO_2 system. On the Fig. 6, four isotherms at temperatures higher than the CO_2 critical temperature are represented with the mixture critical line. The values of the mixture critical points are listed in Table VIII. NRTL and WS parameters have been fitted either on experimental data (CO_2 – R32 and R32 – SO_2) or on the PSRK predicted values (CO_2 – SO_2) in order to calculate the three-component mixture critical line. Then, the mixture critical line is predicted using our in-house software. The predicted critical values for this mixture are reported in Table X, and Fig. 8 shows the PT diagram of this ternary system.

5. CONCLUSION

In this paper, we present VLE data for the $\text{R32} + \text{SO}_2$ system at eight temperatures. We used a static–analytic method to obtain our experimental data. We chose the Peng–Robinson EoS, with the Mathias–Copeman alpha function and the Wong–Sandler mixing rules involving the NRTL model to fit experimental data.

Table X. Three Components CO₂ (1)–R32 (2)–SO₂ (3) Mixture Critical Points

x_1	T_{cal} (K)	P_{cal} (MPa)	x_2
0.1	348.25	6.196	0.9
0.1	357.97	6.671	0.8
0.1	366.98	7.108	0.7
0.1	375.63	7.493	0.6
0.1	383.97	7.823	0.5
0.1	392.01	8.095	0.4
0.1	399.76	8.308	0.3
0.1	407.25	8.465	0.2
0.1	414.48	8.570	0.1
0.1	422.20	8.701	0.0
0.2	344.47	6.553	0.8
0.2	354.72	7.096	0.7
0.2	363.87	7.599	0.6
0.2	372.61	8.041	0.5
0.2	380.97	8.420	0.4
0.2	389.00	8.733	0.3
0.2	396.70	8.984	0.2
0.2	404.11	9.177	0.1
0.2	412.43	9.442	0.0
0.5	331.09	7.411	0.5
0.5	341.35	8.190	0.4
0.5	350.84	8.918	0.3
0.5	359.52	9.535	0.2
0.5	367.47	10.048	0.1
0.5	375.35	10.494	0.0
0.7	320.68	7.598	0.3
0.7	329.05	8.425	0.2
0.7	338.51	9.220	0.1
0.7	346.29	9.633	0.0

The experimental results are given with the following uncertainties: ± 0.02 K, ± 0.0015 MPa, and $\pm 1\%$ for vapor and liquid mole fractions. The particular discontinuity at the R32 critical temperature of the adjusted parameters confirms what was observed in previous studies. Finally, predicted mixture critical lines are presented for this system and the CO₂–R32–SO₂ ternary system.

NOMENCLATURE

- a Parameter of the equation of state, energy parameter ($\text{J} \cdot \text{m}^3 \cdot \text{mol}^{-2}$)
 A Helmholtz energy ($\text{J} \cdot \text{mol}^{-1}$)

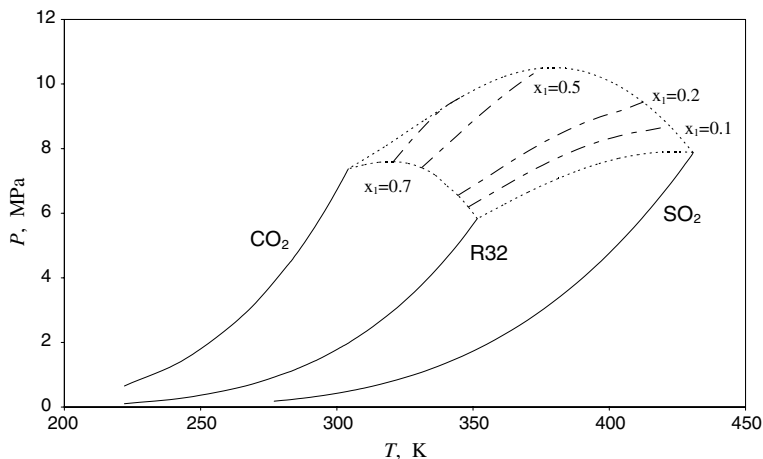


Fig. 8. PT diagram for the CO₂ (1)-R32 (2)-SO₂ (3) system; ·····, predicted binary mixture critical line; -.-.-, predicted ternary mixture critical line.

- b* Parameter of the equation of state, molar co volume parameter ($\text{m}^3 \cdot \text{mol}^{-1}$)
- c* Mathias–Copeman coefficient
- C* Numerical constant
- F* Objective function
- g* Molar Gibbs energy ($\text{J} \cdot \text{mol}^{-1}$)
- k_{ij}* Binary interaction parameter
- P* Pressure (MPa)
- R* Gas constant ($\text{J} \cdot \text{mol}^{-1} \cdot \text{K}^{-1}$)
- T* Temperature (K)
- x* Liquid mole fraction
- y* Vapor mole fraction
- Z* Compressibility factor

Greek Letters

- α_{ij} NRTL model parameter, Eq. (6)
- τ_{ij} NRTL model binary interaction parameter, Eq. (6) ($\text{J} \cdot \text{mol}^{-1}$)
- ω Acentric factor
- μ Molar chemical potential ($\text{J} \cdot \text{mol}^{-1}$)
- ΔU Deviation, $U_{\text{exp}} - U_{\text{cal}}$

Superscript

- E* Excess property
- 0* Initial state

Subscripts

C	Critical property
cal	Calculated property
exp	Experimental property
<i>i, j</i>	Molecular species
∞	Infinite pressure reference state

REFERENCES

1. A. Valtz, C. Coquelet, A. Baba-Ahmed, and D. Richon, *Fluid Phase Equilib.* **202**:29 (2002).
2. A. Valtz, C. Coquelet, A. Baba-Ahmed, and D. Richon, *Fluid Phase Equilib.* **207**:53 (2003).
3. C. Coquelet, A. Chareton, A. Valtz, A. Baba-Ahmed, and D. Richon, *J. Chem. Eng. Data* **48**:317 (2003).
4. C. Coquelet, D. Nguyen Hong, A. Chareton, A. Baba-Ahmed and D. Richon, *Int. J. Refrig.* **26**:559 (2003).
5. F. Rivollet, A. Chapoy, C. Coquelet, and D. Richon, *Fluid Phase Equilib.* **218**:95 (2004).
6. A. Valtz, C. Coquelet, and D. Richon, *Fluid Phase Equilib.* **220**:75(2004).
7. S. Laugier and D. Richon, *Rev. Sci. Instrum.* **57**:469 (1986).
8. P. Guilbot, A. Valtz, H. Legendre, and D. Richon, *Analisis* **28**:426 (2000).
9. D. Y. Peng and D. B. Robinson, *Ind. Eng. Chem. Fundam.* **15**:59 (1976).
10. P. M. Mathias and T. W. Copeman, *Fluid Phase Equilib.* **13**:91 (1983).
11. D. S. H. Wong and S. I. Sandler, *AIChE J.* **38**:671 (1992).
12. H. Renon and J. M. Prausnitz, *AIChE J.* **14**:135 (1968).
13. E. R. Åberg and A. G. Gustavsson, *Analytica Chimica Acta* **144**:39 (1982).
14. A. Chapoy, C. Coquelet, and D. Richon, *Fluid Phase Equilib.* **214**:101 (2003).
15. R. A. Heidemann and A. M. Khalil, *AIChE J.* **26**:769 (1980).
16. M. L. Michelsen and R. A. Heidemann, *AIChE J.* **27**:521 (1981).
17. R. Stockfleth and R. Dohrn, *Fluid Phase Equilib.* **145**:43 (1998).
18. T. Holderbaum and J. Gmehling, *Fluid Phase Equilib.* **70**:251 (1991).
19. Dortmund Data Bank (DDB) Version 97; DDBST Software and Separation Technology GmbH, Oldenburg, Germany (1997).
20. R. C. Reid, J. M. Prausnitz, and B. E. Poling, in *The Properties of Gases and Liquids*, 4th edn. (McGraw-Hill, New York, 1987).